Chapter 5

Coherent scattering of microwaves by particles: Evidence from clouds and smoke

Abstract. *Many radar measurements of the atmosphere can be explained in terms of two scattering mechanisms: incoherent scattering from particles, and coherent scattering from variations in the refractive index of the air, commonly called clear-air or Bragg scattering. Spatial variations in the liquid water content of clouds may also give a coherent contribution to the radar return, but it is commonly believed that this coherent scattering from the droplets is insignificant, because variations in humidity have a much larger influence on the refractive index than equal variations in liquid water content. We argue that the fluctuations in water vapour mixing ratio in clouds can be much smaller than those in liquid water mixing ratio.*

In this chapter an expression for the strength of the coherent scattering from particles will be derived for fluctuations caused by turbulent mixing with clean (i.e., particle-free) air, where it will be assumed that the particles follow the flow, i.e., their inertia is neglected. It will be shown that the coherent contribution adds to the incoherent contribution, the latter always being present. The coherent particle scattering can be stronger than the incoherent scattering, especially at longer wavelengths and high particle concentrations.

Recently published dual-frequency measurements of developing cumulus clouds and smoke show a correlation for which no explanation has been found in terms of incoherent particle scattering and coherent air scattering. Scatterplots of the reflectivity factors at both frequencies show a clustering of points in between the values that correspond to pure clear-air and pure incoherent scattering. Those differences in the radar reflectivity factors could be due to a mixture of Bragg scattering and incoher-

ent particle scattering, but then no correlation is expected, because the origin of the scattering mechanism that dominates at each wavelength is different.

However, coherent scattering from the particles can cause the radar reflectivities of dual-wavelength radar measurements to become correlated with each other. It may explain the slopes and the differences seen in the scatter plots of the radar reflectivities of cloud and smoke measurements, with reasonable values of the parameters involved. However, the correlation between the radar reflectivities is very tight near the cloud top and seems to be present in adiabatic cores as well. This is an indication that, apart from mixing with environmental air, the inertia of the droplets could also be important for the creation of small-scale fluctuations in droplet concentration.

5.1 Introduction

The field of cloud research develops rapidly at the moment, because climate researchers need more knowledge on clouds to understand how the climate changes as a result of human activities. The cloud feedback in different climate models causes a large part of the differences found in the predictions of future climates [Kattenberg et al., 1996]. Radar plays a unique role in cloud research, as it is the only remote sensing instrument that can measure inside dense clouds. To be able to use the radar measurements in a quantitative way, one must understand the scattering mechanisms involved very well.

Two mechanisms explain most of the reflections measured by radar in the troposphere: incoherent scattering, caused by randomly moving particles, and coherent air scattering, caused by variations in the refractive index of the air. Radar measurements of particles are normally performed in the Rayleigh regime, i.e., with a radar wavelength that is much larger than the particle size. Incoherent scattering in the Rayleigh regime by particles of a given size decreases strongly with radar wavelength. With increasing wavelength, the strength of both the incoherent and the coherent scattering decrease, but the incoherent Rayleigh scattering decreases at a much faster rate (see, e.g., Ottersten (1969)).

Coherent backscattering is caused by spatial variations in the atmospheric radio refractive index on a scale of half the wavelength. The fluctuations in the refractive index of the air can result from fluctuations in water vapour content, temperature and pressure. This coherent scattering from the air is usually called Bragg scattering or clear-air scattering, but these terms are somewhat deceptive. The mechanism is similar to that observed in Bragg scattering from crystals' lattices, but not exactly the same. Also, coherent scattering from fluctuations in the refractive index of the air can occur in clouds, so then the term clear-air scattering is misleading. We will there-

fore denote the coherent scattering from fluctuations in refractive index of the atmospheric gases by *coherent air scattering*.

Spatial variations in the mass concentration of particles can cause *coherent particle scattering*, in a way similar to that of coherent air scattering. This coherent particle scattering was long thought to be insignificant in clouds. Gossard (1979) has calculated that in a cloud, coherent air scattering should be 30 times as strong as coherent droplet scattering, under the assumption that the variations in the density of water vapour and liquid water, when expressed in the same units, are about equal. However, in this chapter it will be made plausible that variations in liquid water density inside clouds can be much larger than those in water vapour density. Furthermore, it will be argued that a correlation between the X-band and the S-band reflectivity factor in simultaneous measurements of developing cumulus clouds performed by Knight and Miller (1998) may be explained by the presence of coherent scattering from the droplets**,** although the explanation may not be complete yet. Rogers and Brown (1997) observed a correlation between the X-band and UHF radar reflectivities in dual-wavelength radar measurements of a smoke plume caused by an intense industrial fire. It will be shown that the coherent scattering theory may explain this correlation as well.

The outline of this chapter is as follows. In section 5.2, the scattering of radio waves by a volume with particles is discussed and an equation expressing the strength of the coherent backscattering is derived for the case that the spatial fluctuations are caused by turbulent mixing with particle-free air. The measurements of clouds are described and analysed in section 5.3, while those of the smoke are considered in section 5.4. Section 5.5 discusses the material presented in the earlier sections.

5.2 Scattering of radio waves

5.2.1 Coherent air scattering

The theory of scattering from turbulent fluctuations in the refractive index of the air is well developed. The radar cross section per unit volume η (*radar reflectivity*) is given by [Ottersten, 1969]:

$$h = \frac{p^2}{2} k^4 j_n(\mathbf{k}) \tag{5.1}$$

$\varphi_n(\boldsymbol{k})$ is the space spectrum, i.e., the Fourier transform of the three-dimensional spatial covariance function of refractive index fluctuations. The vector $\boldsymbol{k}$ is the wave number vector in the radar radial direction. Its absolute value is related to the radar wavelength l through $k=4\pi/\lambda$. Equation (5.1) expresses that the radar sees a narrow continuum of fluctuations on spatial scales around $\lambda/2$. (Not λ, but $\lambda/2$, because

*back*scattering is considered.) When the fluctuations are distributed isotropically in space, $\varphi_n(\boldsymbol{k})$ does not depend on the direction of $\boldsymbol{k}$. For homogeneous isotropic turbulence there exists an inertial subrange in which $\varphi_n(k)$ follows a power law [Tatarski, 1961]:

$$j_n(k) = 0.033 C_n^2 \, k^{-11/3} \tag{5.2}$$

where C_n^2 is the *structure parameter* of the refractive index fluctuations and is a measure of the strength of the refractive index variations at all scales. Ottersten (1969) points out some other useful relations for isotropic turbulence, e.g., for the refractive index variance spectrum:

$$E_n(k) = 4p \, k^2 j_n(k) \tag{5.3}$$

En(k) follows the famous "−5/3-law" of Kolmogorov in the inertial subrange. Combining Eqs. (5.1) and (5.2) and substituting $k=4\pi/\lambda$ leads to the well-known expression:

$$h(l) = 0.38 C_n^2 \, l^{-1/3} \tag{5.4}$$

The coherent air scattering from refractive index fluctuations thus has a weak wavelength dependence in the inertial subrange. Variations in water vapour contribute most to the clear-air scattering in the lower atmosphere [Gossard and Strauch, 1981].

Equation (5.4) is valid for radar wavelengths larger than a critical wavelength λ_c, which is defined as $8\pi\eta_0$, where η_0 is the Kolmogorov microscale [Gossard, 1984a]. The Kolmogorov microscale varies over the range 0.4-1.25 mm in cumulus clouds [Shaw et al., 1999], so that λ_c varies over the range 1-3 cm. Under conditions of weaker turbulence λ_c can sometimes become larger than 10 cm [Gossard et al., 1984b; Gage et al., 1999]. The X-band radar wavelength will be sensitive to turbulence in cumulus clouds most of the time, but under conditions of weaker turbulence even S-band radars may measure outside the inertial subrange.

5.2.2 Particle scattering

If the wave transmitted by a radar goes through a volume containing particles, part of the energy is scattered back to the radar. The waves scattered back by the particles interfere with each other. If the particles are randomly spaced, then some configurations of particle positions will show a net constructive interference, while other configurations have a net destructive interference, but, on average, the interference is zero. The received power, when averaged over all possible configurations of the particle positions, is equal to the sum of the powers scattered back by the individual particles. There is no net interference and one speaks of *incoherent scattering*. The radar reflectivity for incoherent scattering from a volume V with N_v small spherical particles is given by [Battan, 1973]:

$$h = \frac{p^5 |K|^2}{l^4} \frac{1}{V} \sum_{i=1}^{N_v} D_i^6 \tag{5.5}$$

This expression is valid for particles with diameters D_i much smaller than the wavelength λ. $K = (\varepsilon_r - 1)(\varepsilon_r + 2)^{-1}$, a constant that is determined by the relative permittivity of the particles (ε_r); ($|K|^2$ equals 0.93 for water and a wavelength of 10 cm.)

When the particles are not completely randomly positioned, a net interference may result and the radar reflectivity differs from Eq. (5.5). Several scattering theories are known in the literature that take interference into account. Two of these will be briefly reviewed below and compared with each other. They mainly differ in their way of modeling the coherent scattering.

Siegert and Goldstein (1951) treat the backscattering from ensembles of scatterers. For simplicity they assume that all the scattering particles return a signal of equal magnitude. Defining $N(r)dr$ as the number of scatterers between a distance r and $r+dr$ from the radar, they derive the following formula for the cross section σ:

$$s = |p|^2 \int_0^\infty \bar{N}(r)dr + |p|^2 \left| \int_0^\infty \bar{N}(r) e^{-ikr} dr \right|^2 \tag{5.6}$$

In this equation, p is a proportionality constant that is assumed to be the same for all scatterers, k equals $4\pi/\lambda$, and the overbar denotes a time average. The first term is the *incoherent* contribution to the cross section. It results from the assumption that the scatterers are independent, at least in the sense that the presence of a certain scatterer in any interval does not prejudice the presence of other scatterers. The second term in Eq. (5.6) is called the *coherent* term. It expresses the coherent contribution to the cross section due to *deterministic* spatial variations in the concentration. For example, the backscattering due to large-scale gradients is included in this term. This term equals zero if the time-averaged concentration has no fluctuation on a spatial scale of half the wavelength. The term could be important when, for example, there are sudden spatial changes in refractive index of the atmosphere. The treatment of Siegert and Goldstein is incomplete in the sense that Eq. (5.6) does not include the coherent scattering from spatial fluctuations caused by, for example, turbulent mixing. Turbulent mixing can cause the scatterer concentration to vary both in space and time. This means that the time average of the concentration can be a constant, i.e., independent of position, but still at any particular time there can be a spatial correlation in the concentration, just as there can be a correlation in the values that the concentration has in time, at any given position. The spatial correlation can cause a coherent return. This fact is not included in Eq. (5.6).

Gossard and Strauch (1983) do take spatial correlations in concentration into account. Let $N(\mathbf{r})d\mathbf{r}$ be the number of drops in the position increment between $\mathbf{r}$ and $\mathbf{r}+d\mathbf{r}$. The radar backscattering is proportional to a factor I, which is given by:

$$I = \overline{\left| \int N(\mathrm{r}) \exp(-\mathrm{i}\,\mathrm{k} \cdot \mathrm{r})\, \mathrm{dr} \right|^2} \tag{5.7}$$

The overbar denotes a time average. For backscattering, the wave-number vector $\boldsymbol{k}$ has an absolute value equal to $4\pi/\lambda$ and is directed from the scatterers to the radar. It is again assumed for simplicity that all the scatterers have the same cross section. Gossard and Strauch split $N(\boldsymbol{r})$ into two terms, a deterministic and a random part: $N = N(\mathrm{r}) + dN(\mathrm{r})$. The deterministic part gives a contribution identical to the second term on the right-hand side of Eq. (5.6) and will here be further ignored. The random part has a time average which is zero and gives the contribution:

$$I = \iint \overline{dN(\mathrm{r})\,dN(\mathrm{r}+\mathrm{l})}\,\mathrm{dr}\exp(-\mathrm{i}\mathrm{k}\cdot\mathrm{l})\,\mathrm{dl} \tag{5.8}$$

If a spatial correlation function is defined as follows:

$$C(\mathrm{l}) = \frac{1}{V\cdot\overline{dN^2}}\int_V \overline{dN(\mathrm{r})\,dN(\mathrm{r}+\mathrm{l})}\,\mathrm{dr} \tag{5.9}$$

where V is the scattering volume, then Eq. (5.8) can be expressed as:

$$I = V\,\overline{\delta N^2}\int C(\boldsymbol{l})\exp(-\mathrm{i}\boldsymbol{k}\cdot\boldsymbol{l})\,\mathrm{d}\boldsymbol{l} \tag{5.10}$$

The integral in Eq. (5.10) is a Fourier integral and I can be written in terms of the three-dimensional spectrum $\varphi_N(\boldsymbol{k})$ of concentration fluctuations as follows:

$$I = (2\pi)^3 V\varphi_N(\boldsymbol{k}) \tag{5.11}$$

Gossard and Strauch argue that if there is no spatial correlation between neighbouring parcels, the backscattered power is proportional to the total number of scatterers in the scattering volume; the usual incoherent return. This is due to the fact that the number of scatterers in a parcel has a Poisson distribution and this distribution has a variance equal to the mean. The incoherent scattering is the same as the first term in Eq. (5.6). If there is a correlation between the concentrations in parcels that are a certain distance apart, then there will be a coherent contribution to the scattering expressed by Eq. (5.11), which we call the *stochastically coherent* contribution. Its strength depends on the amount of fluctuations on scales close to half a wavelength.

Gossard and Strauch do not mention that the incoherent term is always present, even when there is correlation between concentrations in neighbouring parcels [Erkelens et al., 1999a]. This is caused by the fact that the scatterers do not form a continuum, but are discrete points in space. The scatterer concentration is a function of space and time. Neglecting any large-scale gradients, there is a global mean of the concentration for the entire scattering volume. A process such as turbulent mixing can cause fluctuations in the concentration around the global mean. These fluctuations vary in space and time and show correlation between different parcels. Even when the total number of scatterers in a certain parcel is correlated with the total number in a parcel nearby, the exact position of each *individual* scatterer in the parcel

is random (unless the mutual distances between the particles are completely specified, but that is a deterministic case). Therefore, the number of scatterers in *small* parcels with dimensions of the order of the average distance between the scatterers or smaller has a Poisson distribution with an (ensemble) variance equal to the local expected number of scatterers in the parcels. This local expected value is determined by the physical process that creates the correlations between the number of particles in different parcels. In other words, the turbulence or some other physical process causes correlations between the particle concentrations of the parcels, but on top of that we have the Poisson statistics associated with the random nature of the individual scatterer positions. (This means that the total variance of the number of scatterers in a certain volume is larger than one would expect for completely randomly distributed scatterers, i.e., the scatterer distribution exhibits super-Poissonian variance. Kostinski and Jameson (2000) introduced super-Poissonian variance to describe variations in clouds.)

The incoherent backscattering, due to the random positions of the individual particles, and the coherent backscattering, due to the spatial correlations in locally mean scatterer concentration, are additive. Equation (5.11) describes the coherent backscattering for which the theory for scalar conservative passive additives in homogeneous, isotropic turbulence predicts a $k^{-11/3}$ dependence [Tatarski, 1961]. However, in the theory the concentration is considered as a continuous function in space and time. As explained above, the discrete nature of the particles is the cause why the usual incoherent scattering is also present, in addition to the coherent scattering.

5.2.3 Radar Reflectivity Factor

In this section an expression is derived for the total radar reflectivity factor for the case where fluctuations are caused by turbulent mixing and the particles can be considered as *conservative passive additives*.

The presence of scatterers changes the refractive index of a vacuum. If the particles are small compared with the wavelength, then the refractive index n of the medium as a whole is approximated by (see, e.g., Van de Hulst (1981), page 67):

$$n = 1 + 2\pi\alpha N \tag{5.12}$$

where N is the concentration of scatterers and α the polarizability of the scatterers. For small spheres, the polarizability is given by (Van de Hulst (1981), page 70):

$$\alpha = \frac{1}{8}\frac{\varepsilon_r - 1}{\varepsilon_r + 2} D^3 = \frac{1}{8} K D^3 \tag{5.13}$$

where ε_r is the permittivity of the material of the scatterer. The variance of the refractive index due to variations in scatterer mass concentration is given by:

$$\operatorname{var} n = \frac{\pi^2}{16} |K|^2 \operatorname{var}(ND^3) \tag{5.14}$$

To find an expression for the radar reflectivity for the coherent scattering, var n has to be related to C_n^2 and an expression for var(ND^3) is needed. For this, we make use of the fact that the three-dimensional spectrum of isotropic refractive index fluctuations is normalised such that [Ottersten, 1969]:

$$\int_0^\infty 4\pi k^2 \varphi_n(k)\, dk = \operatorname{var} n \tag{5.15}$$

If it is assumed that: 1) there are no variations on scales larger than L_0, the outer scale of the inertial subrange, and 2) the inner scale is much smaller than the outer scale, then, putting Eq. (5.2) into Eq. (5.15) and integrating from $2\pi/L_0$ to infinity, leads to [Gage and Balsley, 1980]:

$$C_n^2 = 5.5\, L_0^{-2/3} \operatorname{var} n \tag{5.16}$$

Because we want to derive an expression for the *coherent* contribution to the radar reflectivity factor, fluctuations in n due to the random positions of the individual particles are ignored for now. As explained in section 5.2.2, these fluctuations give rise to the usual incoherent scattering term.

Suppose there are two volumes with air containing different concentrations of scatterers, and the scatterers are randomly distributed. If the volumes are mixed by turbulence, spatial fluctuations in the concentration are generated. The strength of the fluctuations will be larger when the difference in initial concentrations is larger. In the extreme case that one of the volumes contains all the scatterers and the other none, both the mean concentration and the amplitude of fluctuations in the mixing region are proportional to the initial concentration. This may occur, for instance, in the case of mixing of cloudy air with clean air, as happens at the sides and top of convective clouds. One can assume that the standard deviation in the mass concentration of scatterers is proportional to the mean mass concentration, with a factor of proportionality that will be called β (i.e., the *relative standard deviation* of the mass concentration). It depends on the ratio of the volumes of environmental and cloudy air that mix, and on the rate with which fluctuations are created and removed. For the variance one can write $\operatorname{var}(ND^3) = b^2 (\bar{N})^2 D^6$, where it has been assumed for simplicity that all scatterers have the same diameter D. Equation (5.5) shows the incoherent radar reflectivity and combining Eqs. (5.4), (5.14), and (5.16) gives the coherent radar reflectivity. Combining incoherent and coherent terms and multiplying by $\lambda^4/\pi^5 |K|^2$ gives the total *radar reflectivity factor Z*:

$$Z = \bar{N} D^6 + 4.2\times 10^{-3} L_0^{-2/3} b^2 (\bar{N})^2 D^6\ l^{11/3} \tag{5.17}$$

The coherent backscattering depends on the square of the concentration. The incoherent radar return depends linearly on the concentration. Both the incoherent and coherent returns depend on the diameter to the power of six. The coherent term in Eq. (5.17) becomes increasingly important for longer wavelengths and higher particle densities. If we consider the following range of values of the parameters:

β: 0.05–1 (see section 5.3.2), L_0: 10–500 m, and N: 100–1000 cm^{-3}, then the ratio of the coherent to the incoherent term of Eq. (5.17) spans the following range: for a wavelength of 3 cm the ratio lies between −44 dB and +4 dB, for 10 cm between −24 dB and +23 dB, and for 30 cm between −7 dB and 40 dB. Hence, coherent particle scattering might in some cases be significant at X-band, it can very well be important at S-band, and even more so for UHF radars.

Equation (5.17) is applicable when the fluctuations in particle concentration are caused by mixing between air volumes having large differences in concentration. Several recent studies show that fluctuations in particle concentration can appear in turbulent flows due to the inertia of the particles, without the need for mixing with air with a different mean concentration (see, e.g., Squires and Eaton (1991), Vaillancourt (1998), Shaw et al. (1999)). The particles are preferentially concentrated by coherent turbulent structures. The importance of the effect in clouds is, however, still under debate (see, e.g., Grabowski and Vaillancourt (1999)). The fluctuations that are found with this *preferential concentration mechanism* generally appear on scales of a few centimetres. The mechanism works for a limited range of particle masses: very light particles just follow the flow, while for heavier particles gravitational sedimentation becomes important. If the particles are too heavy, they just fall through the turbulent structures and there is not enough interaction. The total radar reflectivity factor for a volume where the preferential concentration mechanism is operating will also have an incoherent component $\overline{N}D^6$ and a coherent component proportional to $(\overline{N})^2 D^6$, but the wavelength dependence and the strength of the coherent component could differ much from Eq. (5.17).

5.2.4 Dual-frequency measurements

If dual-frequency measurements of purely coherent scattering are compared, a difference between the measured radar reflectivities will be found. If both wavelengths fall within the inertial subrange, this difference can be calculated from:

$$Z_1 = Z_2 + 10 \cdot \log\left(\frac{l_1}{l_2}\right)^{11/3} \tag{5.18}$$

Z_1 and Z_2 are the reflectivity factors for the two wavelengths, expressed in dBZ, and *log* is the logarithm of base 10. For example, in sections 5.3 and 5.4 dual-wavelength measurements of developing cumulus clouds and smoke are discussed. The wavelengths used are 3 cm and 10 cm for the clouds and 3.2 cm and 33 cm for the smoke. Equation (5.18) predicts differences of 19 dBZ and 37 dBZ for purely coherent scattering for these pairs of wavelengths.

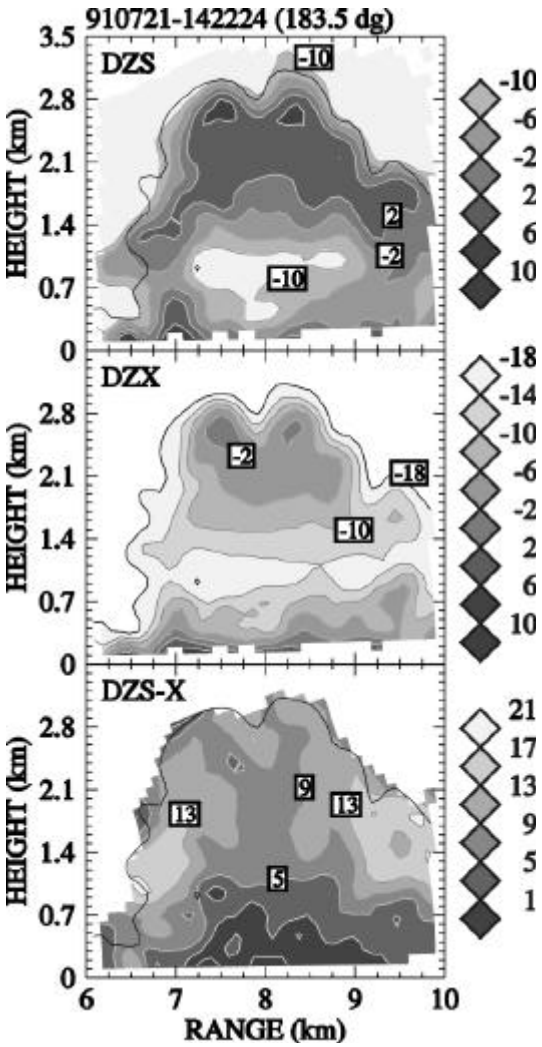

Figure 5.1. An example of a developing cumulus cloud. DZS and DZX are the S-band and X-band reflectivity factors, respectively, expressed in dBZ. DZS-Z is their difference. DZS shows a large weak-echo region near cloud base and some signs of a mantle echo. DZX shows very clear flat echo bases. (Fig. 12 from Knight and Miller (1998))

Dual-frequency measurements of purely incoherent scattering by small spheres should by definition give a difference of 0 dB. If both incoherent and coherent scattering contribute to the return, the measured difference should lie somewhere between 0 dBZ and the value predicted by Eq. (5.18). This happens, for example,

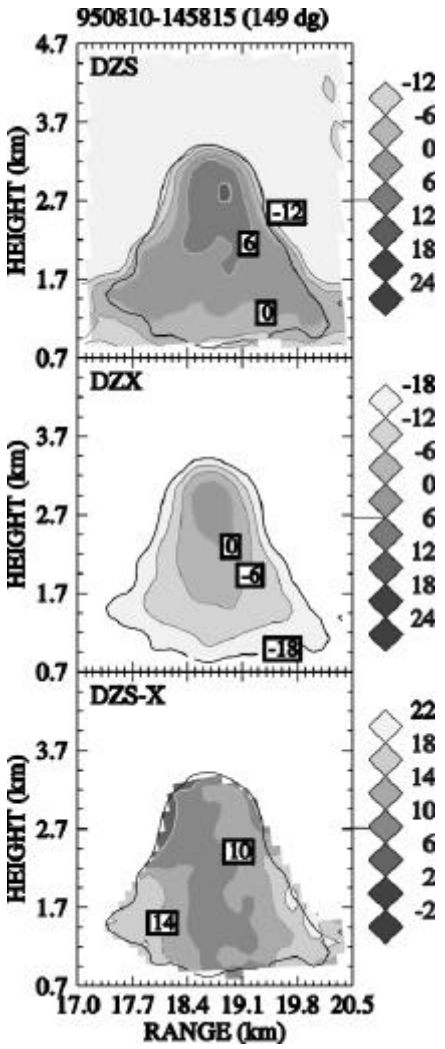

Figure 5.2. A developing cumulus cloud, showing a strong correlation between DZS and DZX, which cannot be explained in terms of the traditional scattering mechanisms of incoherent particle scattering and coherent air scattering. DZS-X is near 10 dBZ in a large part of the cloud. (Fig. 10 (c) from Knight and Miller (1998)).

when the radar return at the longer wavelength is dominated by coherent scattering from humidity and temperature variations and the return at the shorter wavelength by incoherent scattering from particles.

Values between the limits are observed for the majority of the measurements of developing cumulus clouds [Knight and Miller, 1998], and for smoke [Rogers and

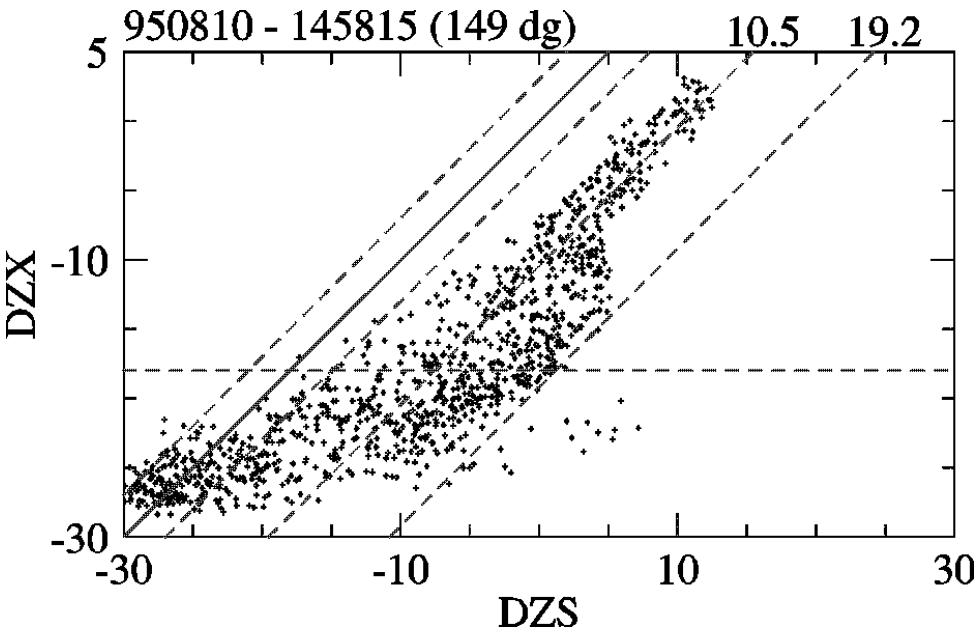

Figure 5.3. Scatterplot of DZS versus DZX for the cloud of Fig. 5.2. The dotted horizontal line at –18 dBZ is a conservative value of the noise level of the X-band radar (Figure 11(c) from Knight and Miller (1998)).

Brown, 1997]. The puzzling aspect of these measurements is that both sets of measurements show a correlation between the reflectivity factors at two wavelengths, which one does not expect when the origins of the radar returns are different. The measurements will be discussed further in the following sections.

5.3 Dual-wavelength measurements of cumulus clouds

5.3.1 Description of the measurements

In a recent article, Knight and Miller (1998) discuss measurements of developing cumulus clouds, performed with 2 radars: an X-band radar with a wavelength of 3-cm and an S-band radar with a wavelength of 10 cm. Two examples are shown in Figs. 5.1 and 5.2. The measurements were obtained during the CaPE and SCMS campaigns, Florida, in July and August 1991 and 1995. In these figures, DZS, DZX and DZS-X denote the radar reflectivity factor at S-band, at X-band and their difference, respectively. Most measurements could be explained by the traditional theory. For example: Coherent air scattering at the borders of the cumulus clouds is due to

mixing of the humid cloudy air with dryer environmental air and can cause *mantle echoes* with differences in the reflectivity factors close to 19 dBZ, the value expected for coherent scattering at these wavelengths; or, when drizzle or rain droplets are present, the Rayleigh scattering from them can dominate, causing equal reflectivity factors. In these cases there is a correlation in the returns, as the scattering process dominating both wavelengths is the same. Also cases were observed in which the 10-cm radar measured coherent scattering, while the 3-cm radar measured incoherent scattering, and there was no correlation between the reflections.

However, often there was a correlation in the X- and S-band reflectivity factors, but their difference was not equal to 0 dBZ (the value for purely incoherent scattering) or 19 dBZ (for purely coherent scattering). For example, in Fig. 5.3 some of the X- and S-band reflectivity factors lie on a line with a slope of one with a difference of about 10 dBZ (but other offsets have been observed as well). No simple explanation for this can be found from the conventional theories of incoherent droplet scattering and coherent air scattering. The phenomenon was especially noticeable on days where the air outside the cloud was very humid, because the effect was not obscured then by coherent scattering due to water vapour fluctuations at the borders of the cloud. In section 5.3.2, a possible explanation for this correlation will be presented in terms of coherent scattering from the droplets.

At the cloud bases of the developing cumulus clouds, Knight and Miller reported two important features: *flat echo bases* and *weak-echo regions*. Flat echo bases are occasionally observed; they are very flat and horizontal bottoms in the X-band echo contours, similar to the visually flat cloud base at the condensation level. Figure 5.1 shows a clear example. Here the S-band reflectivity pattern also shows a flat echo base, but this is not always the case. Knight and Miller interpret the flat echo bases as the result of unmixed adiabatic ascent.

The base of the cloud in Fig. 5.1 is probably somewhere between 400 m and 700 m. Near the cloud base the S-band measurement shows a region with lower reflectivities. This region is called *weak-echo region* and is seen in nearly all the actively growing clouds. The bottom frame shows that the S-band reflectivity is dominated by coherent scattering, so the weak-echo region is a minimum in the coherent return at S-band. It is also sometimes present at X-band, but is then much less pronounced. The weak-echo region at S-band extends almost to the ground here. The weak-echo regions often have reflectivity factors in the order of -20 dBZ.

Another feature reported by Knight and Miller is that on some days it is fairly common that the difference in reflectivity factors in the mantle echoes is not 19 dBZ, but several dBs higher. This indicates a slope steeper than -5/3 for the variance spectrum of the refractive index variations. It may be that the X-band radar measured in the dissipation range, but a steeper slope may also be due to the effect of evaporation and condensation on the slope of the variance spectrum of humidity variations, as will be explained in section 5.3.3.

5.3.2 Coherent particle scattering in cumulus clouds

This section will show quantitatively that coherent droplet scattering in cumulus clouds can be significant compared to incoherent droplet scattering, and that coherent droplet scattering may explain the correlation in X- and S-band reflectivities that was found in the measurements of the developing cumulus clouds.

For the 10-cm radar used in the cumulus study Eq. (5.17) becomes:

$$Z(10\text{ cm}) = \bar{N}D^6 + 9.0\times10^{-7}\, b^2\, L_o^{-2/3}(\bar{N})^2 D^6 \tag{5.19}$$

In-situ aircraft measurements of the droplet concentrations performed during CaPE in clouds very similar to the ones described above showed droplet concentrations reaching 800-900 cm^{-3} near cloud base [Paluch et al., 1996]. There is much uncertainty about the values of β and L_0, and they may be related. A value of 10 m for L_0 was used by VanZandt et al. (1978) for the free atmosphere, but this value is probably much too small for the developing cumulus clouds considered here. Davis et al. (1996) measured the spatial fluctuations of liquid water content in marine stratocumulus clouds using a King hot-wire probe and Davis et al. (1999) used a Particulate Volume Monitor for that purpose in broken stratocumulus decks with embedded towering cumulus. By dividing the standard deviation of the liquid water content measurements by their mean value, an estimate of the relative standard deviation β is obtained. This yields values between 0.05 and 0.58. A difference in the reflectivity factors of about 10 dBZ has been observed. Such a difference would result for example for L_0=150 m and β=0.6. This result shows that coherent droplet scattering *can be significant* in S–band measurements of cumulus clouds. In Fig. 5.2, the strongest correlation between the radar reflectivity factors at X-band and at S-band occurs for values of the X-band reflectivity factor that lie between about -5 dBZ and 2 dBZ. For a concentration of 800 cm^{-3}, this would mean droplet diameters between 27 μm and 35 μm (when the droplet size distribution is assumed to be mono-disperse).

Since both the incoherent term and the coherent term in Eq. (5.19) depend on D^6, we could explain the observed correlation by assuming that the differences between the measured data points are mainly due to an increase in the average diameter of the particles with height: the ascending air becomes colder and the droplets grow because of condensation.

Fluctuations on scales of about 5 mm to 5 cm have been found experimentally from FSSP data [Baker, 1992] in cumulus cloud regions which were picked by the eye to be homogeneous on large scales. Such cm-scale fluctuations might be caused by the preferential concentration mechanism mentioned earlier. The coherent scattering from such fluctuations can already be significant for very small values of the relative standard deviation β, if the fluctuations appear only on the small scales and not on larger scales. A very rough estimate can be obtained by assuming that the −5/3 law is valid for these cm-scale fluctuations. Then one may set L_0 in Eq. (5.19) equal to 5 cm

to compute a coherent contribution that is about 10 dB stronger than the incoherent contribution for β as small as 0.04.

5.3.3 Coherent air scattering in clouds

In addition to the incoherent and coherent contributions to the radar reflectivity from particles, the air also supplies a coherent contribution. The refractive index of clear (i.e., particle-free) air depends on pressure, temperature and humidity. Fluctuations in water vapour concentration dominate the scattering by clear air in the lower atmosphere [Gossard and Strauch, 1981]. Gossard (1979) has compared the relative magnitudes of coherent scattering from water vapour fluctuations in clouds with that of coherent scattering from droplets. He derives for the variations in refractive indices n_v (due to vapour variations) and n_l (due to liquid variations):

$$\begin{aligned} \operatorname{var} n_v \times 10^{12} &\approx 58.5 \operatorname{var} Q_v \\ \operatorname{var} n_l \times 10^{12} &\approx 2.09 \operatorname{var} Q_l \end{aligned} \tag{5.20}$$

respectively.

Q_v and Q_l are the water vapour and liquid water mixing ratios (grams per kilogram of dry air) and "var" designates the spatial variance. Gossard and Strauch (1983) state that within a cloud in steady state at saturation with no precipitation removing water from the cloud and minimal entrainment, it seems reasonable to assume that var Q_v is equal to var Q_l. Since the coherent scattering is proportional to var n, the contribution to coherent scattering from water vapour fluctuations is about 30 times stronger than coherent scattering from droplets for equal variations in water vapour content and liquid water content (see Eqs. (5.4) and (5.16)).

There are several mechanisms that influence the strength of the water vapour and liquid water fluctuations [Erkelens et al., 1999b] and it will be argued below that, in clouds, the variations in water vapour can be much smaller than those in liquid water. Consequently, in some cases coherent scattering from the cloud droplets can dominate coherent scattering from water vapour, contrary to common belief.

At the top and sides of convective clouds the cloudy air mixes with environmental air, leading to *mantle echoes* on the reflectivity patterns for longer wavelengths [Knight and Miller, 1998]. The environmental air does not contain water droplets, so mixing can cause large fluctuations in liquid water content. If, in addition, the air outside the cloud is very humid, the resulting fluctuations in the water vapour content can be smaller than those in the liquid water content. Environmental air may penetrate deeply into the cloud, indicated by the thickness of mantle echoes on dry days. The mantle echoes can sometimes be as thick as 1 km at the top of cumulus clouds.

Condensation and evaporation also influence fluctuations in the water vapour content and liquid water content. Condensation and evaporation will always tend to

bring the relative humidity toward about 100% and are more effective for larger deviations from saturation. So this will reduce fluctuations in water vapour content but not necessary the fluctuations in liquid water content. Rogers et al. (1994) report a case where the clear-air echo of a turbulent layer intensified when light rain fell through the layer. They analyse in detail the effect of evaporation of rain on C_n^2 and conclude that the thermodynamic effect of the rain on the layer is to reduce the reflectivity, contrary to what is observed. We wonder whether a coherent scattering contribution from the smallest rain droplets may cause the observed intensification.

The wavelength dependency of $\lambda^{-1/3}$ in Eq. (5.4) is valid for any *conservative passive additive* (CPA) in homogeneous isotropic turbulence in equilibrium [Tatarski, 1961]. For a CPA, the theory says that the fluctuations are generated at large scales and are passed on completely to smaller scales. Only at the smallest scales they are removed (by molecular diffusion). An interesting effect of condensation and evaporation is that it may affect the slope of the spatial spectrum of water vapour and liquid water fluctuations. (Water vapour content and liquid water content are not CPAs and the "-5/3 law" may not be valid.) Condensation and evaporation tend to reduce fluctuations in water vapour content. (This will happen at all scales, but more strongly at larger scales, because the largest deviations from saturation appear at the largest scales). Due to this sink, not all of the fluctuations will be passed on to smaller scales. This means that the slope of the water vapour spatial spectrum could be steeper than that of a CPA.

An updraft may also reduce humidity fluctuations. If there is a mean upward motion of the air then the relative humidity in initially droplet free air will increase until saturation is reached. Then new droplets may form due to condensation. The cloudy air will remain at saturation, but the droplets will grow due to condensation. So, the effect of an updraft would be to reduce fluctuations in water vapour and at the same time increase fluctuations in liquid water, until saturation is reached in the clear air. This may lead to large fluctuations in liquid water concentration and slopes of the spatial variance spectra that differ from 5/3.

It is interesting to note that changes in the slope of the variance spectra can also occur when chemical reactions take place [Corrsin, 1961; Pao, 1964]. The methods used in these references to compute the changes in the spectra might be applied to the clouds, but that is outside the scope of this work.

There are also experimental indications of a deviation from the 5/3 law. Indications of a flatter slope have been found in a forward scattering experiment performed by Gossard and Strauch (1981). The dual-wavelength measurements of Gage et al. (1999) also show signs of a flatter slope. Davis et al. (1999) performed measurements of the liquid water spatial variance spectrum with a Particulate Volume Monitor in stratocumulus clouds. The spectrum shows a slope that is less steep than 5/3 for scales smaller than a few meters.

Diffusion and sedimentation influence fluctuations in water vapour content or liquid water content as well. Diffusion reduces small-scale fluctuations in water vapour content, but this mechanism is negligible for water droplets. However, fluctuations in liquid water content may be removed by droplet sedimentation. The broader the droplet size distribution is, the larger the differences in fall velocities of the droplets, and the more effective sedimentation is in reducing variations in liquid water content.

All the mentioned processes can influence the strength of the fluctuations in water vapour content and liquid water content. A quantitative estimate of the effects is difficult because each of the processes involved has its own time scale. Estimates for some of the time scales involved can be found in, e.g., [Grabowski, 1993].

Due to the effects discussed above, fluctuations in liquid water content may exist for longer times than those in water vapour content and may be much stronger. They may therefore penetrate the cloud more deeply. Mixing could be effective over larger parts of the clouds than might be concluded on the basis of the thickness of the mantle echo. For, the mantle echo mainly represents the area where fluctuations in water vapour content contribute strongly to the S-band reflectivity. Its apparent thickness, however, depends on the contrast in humidity between the saturated cloudy air and the subsaturated environmental air, on how fast humidity variations are reduced, and on the strength of the incoherent contribution.

Simultaneous measurements on centimetre scales of the water vapour and liquid water concentrations are needed to prove that the fluctuations in water vapour are really much smaller than those in liquid water. For a complete description, also the covariances between humidity, temperature and liquid water content should be measured.

Some experimental evidence exists on the possibility of significant coherent particle scattering. Politovich and Cooper (1988) performed measurements of supersaturation in 147 cloud regions. The average supersaturation was near 0 %, with relative standard deviations of 0.4 % in 80 percent entrained air and 0.1 % in the core of cumulus clouds. The regions giving a high correlation between S- and X-band reflectivities in the article by Knight and Miller (1998) are about 2 km above cloud base. An *adiabatic* cloud with a temperature of 25 degrees Celsius and a pressure of 930 mb at cloud base will have a water vapour content of about 17 g/m^3 and a liquid water content of about 6 g/m^3 at 2 km above cloud base. Equations (5.4), (5.16) and (5.20) show that if coherent particle scatter is to dominate coherent air scatter the spatial standard deviations of the variations in liquid water content should be $\sqrt{(58.5/2.09)} = 5.3$ times as large as those in water vapour content. The measurements of Politovich and Cooper would mean that the relative variations in liquid water content should dominate the scattering when they are above 6 % for the entrained region and about 1.5 % in the core of cumulus clouds. (Lower in the cloud the ratio of water vapour content to liquid water content will be higher, thus coher-

ent *air* scatter will be more important near the cloud base.) Davis et al. (1996, 1999) found relative liquid water variations in stratocumulus clouds between 5 % and 58 % of the mean value. It is therefore very well possible that the coherent droplet scattering is stronger than the coherent air scatter in clouds, except close to the cloud base. Venema et al. (1999) have analysed in more detail for which radar frequencies, how often and in which types of clouds coherent particle scattering may be important.

5.4 Dual wavelength measurements of smoke

5.4.1 Description of the measurements

Another measurement showing a puzzling correlation between the radar measurements at two wavelengths was reported by Rogers and Brown (1997). They measured a smoke plume from a large industrial fire with two vertically pointing radars, a UHF profiler (wavelength 33 cm) and an X-band radar (3.2 cm). The smoke was caused by a burning paint factory, located 10 km away from the radars. The factory was burnt to the ground. The plume was overhead the radars about 20 minutes after the fire started.

With these wavelengths, purely coherent scattering would give a 37 dBZ difference in the reflectivity factors. A scatter plot of the reflectivity factors shows that the majority of the points lie between the 0 dBZ difference line and the 37 dBZ difference line, see Fig. 5.4. There is a correlation between the reflectivity factors of both radars. The points lie roughly on a line of slope one half (a least-squares linear fit gives a slope of 0.4). These measurements may also be explained in terms of coherent particle scattering (section 5.4.2). Curiously, a Vaisala CT-12K ceilometer detected little or nothing of the smoke plume.

5.4.2 Coherent particle scattering in smoke

Rogers and Brown (1997) investigate two possible explanations for the difference in the observed reflectivity factors: 1) the presence of cm-sized particles and 2) a strongly perturbed structure of atmospheric refractivity.

Large particles: There are indications that the smoke plume contained a small number of large particles. These indications are: a grainy pattern of high-resolution X-band reflectivity, a predominance of downward velocities in the order of 1 m/s and the fact that a Vaisala CT-12K ceilometer did not detect the plume. If the particles are so large that the Rayleigh approximation is not valid at X-band, then the UHF reflectivity will exceed the X-band reflectivity. Rogers and Brown show that a very small number of cm-sized particles can explain the magnitude of the differ-

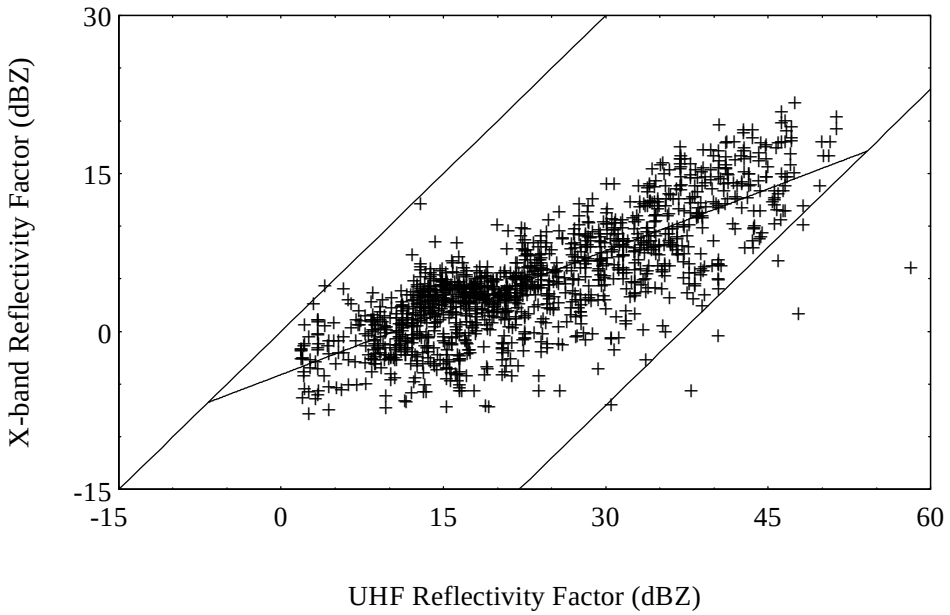

Figure 5.4. Scatterplot of UHF versus X-band reflectivity factors for the smoke measurement described in Rogers and Brown (1997). The reflectivity factors are correlated: they cluster around a line with a slope of about 1/2.

ences that occur if the particles are too large to satisfy the Rayleigh approximation at UHF, but in order to explain the correlation in the measurements the concentration of the particles must increase with their size, which seems unlikely.

It is puzzling that the ceilometer did not detect the plume, because even if the plume contained a small number of large particles, it would probably still contain small particles in much higher concentrations.

Strong clear-air scatter: The heat generated by the fire and gases that are produced could increase the value of C_n^2 to values considerably higher than ordinary observed in the atmosphere, but again it is difficult to explain the correlation.

We suggest that the correlation and the slope near one half can be explained by coherent particle scattering. For wavelengths of 3.2 cm and 33 cm, respectively, Eq. (5.17) becomes:

$$\begin{aligned} Z(3.2\text{ cm}) &= \bar{N}D^6 + 1.4\times10^{-8} b^2 L_o^{-2/3} (\bar{N})^2 D^6 \\ Z(33\text{ cm}) &= \bar{N}D^6 + 7.2\times10^{-5} b^2 L_o^{-2/3} (\bar{N})^2 D^6 \end{aligned} \tag{5.21}$$

Because the first term on the right-hand side of these equations is a linear function of number density and the second term a quadratic function of number density,

there will be some range of values of the number density, where the 3-cm signal is mainly due to incoherent scattering and the 33-cm signal is dominated by coherent scattering. If the number density varies within this range in the plume, then a slope of one half can be produced on a log-log scatter plot of UHF versus X-band reflectivity. Variations in the other variables could be responsible for the considerable scatter in the measurements shown in Fig. 5.4. There is some question about the origin of the variations in concentration. They could be due to spatial and temporal variations in turbulent mixing (in which case one may expect considerable variations in the parameters β and L_0). It could also be that the main variations in concentration are due to variations in the amount of smoke generated by the fire.

The order of magnitude of particle density and diameter can be estimated. If β is taken to be unity and L_0 equal to 10 m, then it can be calculated with Eq. (5.21) that concentrations ranging from 2 cm^{-3} to 60 cm^{-3} and a diameter of about 90 μm are needed to explain Fig. 5.3. This must be considered a very rough estimate, however, because of the uncertainty in the values of the parameters, but the numbers seem reasonable.

It is curious that the ceilometer detected little or nothing of the smoke plume. One would expect this lidar to detect a cloud consisting of particles with the calculated diameters and number densities. It could be that the lidar backscatter from the smoke plume was reduced because the particles were strongly absorbing at the lidar wavelength. Furthermore, the boundaries of the smoke plume are probably much less sharp than those of the bottom of a water cloud, so a significant part of the power may already have been attenuated before the light reached the position with a relatively high backscattering.

5.5 Discussion

Equation (5.17), which expresses the total equivalent radar reflectivity factor for incoherent and coherent scattering from particles, has been derived assuming that the fluctuations in particle mass density are due to the mixing with clean air. Coherent particle scattering may then explain the correlation in the cloud and smoke measurements with particle concentrations and diameters that are reasonable.

However, fluctuations in particle concentration may also arise due to the preferential concentration mechanisms without the need for mixing. The question is: what is the dominating mechanism causing the fluctuations in particle density?

Most of the points in the scatter plot of Fig. 5.4 show differences between X-band and UHF reflectivities that lie between 0 dBZ and 37 dBZ, the limiting values for purely incoherent and purely coherent scattering due to turbulent mixing, respectively. This is an indication that the variations are created at scales considerably

larger than half the wavelength of the UHF radar and thus mixing with clean air is probably the dominating mechanism for creating the fluctuations in smoke density.

For the clouds, the situation is less clear. The correlation in Figs. 5.2 and 5.3 is strongest near the cloud top, where the scattering from the droplets is largest. Mixing with environmental air could be important for the correlation between the X- and S-band reflectivities there, because the top of the cloud is exactly the place where strong mixing takes place as the thick mantle echoes on dry days indicate.

An argument against mixing being a dominant mechanism in the *core* of the clouds is the occurrence of flat echo bases in the lower parts of the clouds at X-band. These are interpreted as unmixed adiabatic ascent. The weak-echo regions at the base of the clouds could also be an indication of that.

The correlation near the top of the cloud in Fig. 5.3 is remarkably strong. Any fluctuations in the parameters β and L_0 would decrease the correlation if the S-band reflectivity is dominated by the second term of (5.17) and the X-band reflectivity by the first term. The combined variations in β, L_0 and concentration should not be larger than about a factor of 3 to explain the high correlation shown in Fig. 5.3. Variations in these parameters would *all* lead to a slope of 1, and a very strong correlation, if *both* DZS and DZX were dominated by coherent scattering. The problem becomes then to explain the 10 dBZ difference between DZS and DZX, which means a slope of the variance spectrum close to zero, at least at cm-scales.

The correlation in Fig. 5.3 is less strong for DZS smaller than about 5 dBZ. DZS−X has values larger than about 10 dBZ, due to the presence of coherent scattering from humidity fluctuations, but also values *smaller* than 10 dBZ are present. Unless this is caused by some artefact such as the presence of insects, it means that the phenomenon causing the peculiar correlation is less important near cloud base.

If the X-band return would also be dominated by coherent scatter, the droplet concentration estimated from a scatter plot of the X-band reflectivity versus height, assuming an adiabatic liquid water profile, would be underestimated, and the droplet diameters would be overestimated. In fact, there is some evidence for this. Knight and Miller estimate a concentration in the order of 100 cm^{-3} in one example, where they assume a narrow, symmetric droplet size distribution. Using an asymmetric distribution, such as a gamma or a lognormal distribution, would increase the estimated value, but an unrealistically broad spectrum has to be assumed to get a value as high as the 800-900 cm^{-3} found with an FSSP in some of the clouds of CaPE [Paluch et al., 1996].

5.6 Summary and concluding remarks

Besides coherent scattering from variations in refractive index of the air (clear-air/Bragg scattering) and incoherent particle scattering (Rayleigh scattering), coher-

ent scattering by ensembles of particles may also be important in explaining radar measurements of the atmosphere. Coherent particle scattering can considerably enhance the reflections from small cloud droplets and aerosols. Scattering from variations in humidity is probably less important in clouds than was thought until now.

In parts of cumulus clouds coherent scattering from the droplets may be a dominating scattering mechanism, especially at long wavelengths. Two possible mechanisms for creating fluctuations in particle mass density have been considered: mixing with environmental air and the preferential concentration mechanism. The former can create fluctuations on a wide range of scales, while the latter is believed to create fluctuations only on small scales. There are indications that coherent droplet scattering is important even at X-band and also in the core of the clouds. This is an indication that the preferential concentration mechanism plays a role. Measuring also with a radar with a longer wavelength would provide information about the range of scales involved, while a radar with a shorter wavelength could tell whether coherent scattering is present at X-band.

Big fires are known to be very efficient radar scatterers [Rogers and Brown, 1997; Banta, 1992]. This may be due to coherent scattering by the smoke particles. Mixing with clean air is likely of importance for creating spatial fluctuations in smoke density.

For the development of a more complete theory of coherent particle scattering, in-situ measurements of fluctuations on small scales are needed. Also simulations with cloud models with a solid physical basis can help improve the understanding of the scattering of radar waves by clouds. Together, theory, measurements and modelling may contribute to an improved understanding of processes in clouds such as turbulence, entrainment and mixing, the evolution of cloud droplet size spectra and warm rain formation.

Acknowledgement

We are indebted to R.R. Rogers, W.O.J. Brown, C.A. Knight and L.J. Miller for useful discussions and providing us with data and figures. We thank W. Klaassen for carefully reading an early version of the manuscript. This research was supported by the Dutch Technology Foundation and the Dutch national research program on global air pollution and climate change.

References

Baker, B.A. Turbulent entrainment and mixing in clouds: a new observational approach. *J. Atmos. Sci.*, **49**, pp. 387-404, 1992.

Banta, R.M., L.D. Olivier, E.T. Holloway, R.A. Kropfli, B.W. Bartram, R.E. Cupp, and M.J. Post. Smoke-column observations from two forest fires using Doppler lidar and Doppler radar. *J. Appl. Met.*, **31**, pp. 1328-1349, 1992.

Battan, L.J. *Radar Observation of the Atmosphere*. University Chicago Press, 324 p., 1973.

Corrsin, S. The reactant concentration spectrum in turbulent mixing with a first-order reaction. *J. Fluid Mech.*, **11**, pp. 407-416, 1961.

Davis, A., A. Marshak, W. Wiscombe, and R. Cahalan. Scale invariance of liquid water distributions in marine stratocumulus. Part I: spectral properties and stationarity issues. *J. Atmos. Sci.*, **53**, pp. 1538-1558, 1996.

Davis, A.B., A. Marshak, H. Gerber, and W.J. Wiscombe. Horizontal structure of marine boundary layer clouds from centimetre to kilometer scales. *J. Geophys. Res.*, **104**, pp. 6123-6144, 1999.

Doviak, R.J., and D.S. Zrnic. *Doppler Radar and Weather Observations*. Academic Press, San Diego, 562 p., 1993.

Erkelens, J.S., V.K.C. Venema, and H.W.J. Russchenberg. Coherent particle scatter in smoke and cumulus clouds. *Proc. IEEE Geosci. and Remote Sensing Symp.*, 28 June 2 July, Hamburg, Germany, pp. 687-689, 1999a.

Erkelens, J.S., V.K.C. Venema, and H.W.J. Russchenberg. Coherent particle scatter in developing cumulus clouds. *Proc. Int. Conf. Radar Meteorology*, American Meteorological Society, 12 16 July, Montreal, Canada, pp. 904-907, 1999b.

Gage, K.S., and B.B. Balsley. On the scattering and reflection mechanisms contributing to clear air radar echoes from the troposphere, stratosphere, and mesosphere. *Radio Sci.*, **15**, pp. 243-257, 1980.

Gage, K.S., C.R. Williams, W.L. Ecklund, and P.E. Johnston. Use of two profilers during MCTEX for unambiguous identification of Bragg scattering and Rayleigh scattering. *J. Atmos. Sci.*, **56**, pp. 3679-3691, 1999.

Gossard, E.E. A fresh look at the radar reflectivity of clouds. *Radio Sci.*, **14**, pp. 1089-1097, 1979.

Gossard, E.E., and R.G. Strauch. The refractive index spectra within clouds from forward-scatter radar observations. *J. Appl. Met.*, **20**, pp. 170-183, 1980.

Gossard, E.E., and R.G. Strauch. *Radar Observation of Clear Air and Clouds*. Elsevier Science Publishers, Amsterdam, 280 p., 1983.

Gossard, E.E., R.B. Chadwick, T.R. Detman, and J.E. Gaynor. Capability of surface-based clear-air Doppler radar for monitoring meteorological structure of elevated layers. *J. Appl. Meteor*, **23**, pp. 474-485, 1984a.

Gossard, E.E., W.D. Neff, R.J. Zamora, and J.E. Gaynor. The fine structure of elevated refractive layers: Implications for over-the-horizon propagation and radar sounding systems. *Radio Sci.*, **19**, pp. 1523-1533, 1984b.

Grabowski, W.W. Cumulus entrainment, fine-scale mixing, and buoyancy reversal. *Q. J. R. Meteorol. Soc.*, **119**, pp. 935-956, 1993.

Grabowski, W.W., and P. Vaillancourt. Comments on 'Preferential Concentration of Cloud droplets by Turbulence: Effects on the Early Evolution of Cumulus Cloud Droplet Spectra.' *J. Atmos. Sci.*, **56**, pp. 1433-1436, 1999. See also reply on pp. 1437-1441.

Kattenberg, A. et al. Chapter 6 in *Climate Change 1995,* J.T. Houghton et al. (Eds.), Cambridge University Press., 1996.

Knight, C.A., and L.J. Miller. Early radar echoes from small, warm cumulus: Bragg and hydrometeor scattering. *J. Atmos. Sci.*, **55**, pp. 2974-2992, 1998.

Kostinski, A.B., and A.R. Jameson. On the spatial distribution of cloud particles. *J. Atm. Sci.*, pp. 901-915, 2000.

Ottersten, H. Radar backscattering from the turbulent clear atmosphere. *Radio Sci.*, **4**, pp. 1251-1255, 1969.

Paluch, I.R., C.A. Knight, and L.J. Miller. Cloud liquid water and radar reflectivity of nonprecipitating cumulus clouds. *J. Atmos. Sci.*, **53**, pp. 1587-1603, 1996.

Pao, Y.-H. Statistical behavior of a turbulent multicomponent mixture with first-order reactions. *AIAA J.*, **2**, pp. 1550-1559, 1964.

Pinsky, M.B., A.P. Khain, and Z. Levin. The role of inertia of cloud drops in the evolution of the spectra during drop growth by diffusion. *Q. J. R. Meteorol. Soc.*, **125**, pp. 553-581, 1999.

Politovich, M.K., and W.A. Cooper. Variability of the supersaturation in cumulus clouds. *J. Atmos. Sci.*, **45**, pp. 1651-1664, 1988.

Rogers, R.R., S.A. Cohn, W.L. Ecklund, J.S. Wilson, and D.A. Carter. Experience from one year of operating a boundary-layer profiler in the center of a large city. *Ann. Geophysicae*, **12**, pp. 529-540, 1994.

Rogers, R.R., and W.O.J. Brown. Radar observations of a major industrial fire. *Bull. Amer. Meteor. Soc.*, **78**, pp. 803-814, 1997.

Shaw, R.A., W.C. Reade, L.R. Collins, and J. Verlinde. Preferential concentration of cloud droplets by turbulence: effects on the early evolution of cumulus cloud droplet spectra. *J. Atmos. Sci.*, **55**, pp. 1965-1976, 1998.

Siegert, A.J.F., and H. Goldstein. Coherent and incoherent scattering from assemblies of scatterers. Appendix B in: *Propagation of short radiowaves*, D.E. Kerr (Ed.), Dover, New York, 1951.

Squires, K.D., and J.K. Eaton. Preferential concentration of particles by turbulence. *Phys. Fluids A,* **3**, no. 5, pp. 1169-1178, 1991.

Tatarski, V.I. *Wave Propagation in a Turbulent Medium*. McGraw-Hill, New York, 285 p., 1961.

Vaillancourt, P.A. Microscopic approach to cloud droplet growth by condensation. Ph.D. dissertation, McGill University, Canada, 174 p., 1998.

Van de Hulst, H.C. *Light Scattering by Small Particles*. Dover, New York, 470 p., 1981.

VanZandt, T.E., J.L. Green, K.S. Gage, and W.L. Clark. Vertical profiles of refractivity turbulence structure constant: comparison of observations by the Sunset radar with a new model. *Radio Sci.*, **13**, pp. 819-829, 1978.

Venema, V.K.C, J.S. Erkelens, H.W.J. Russchenberg, and L.P. Ligthart. Some notes on scattering of radio waves by clouds. *Proc. Symp. Remote Sensing of Cloud Parameters*, 21-22 October, IRCTR, Delft, The Netherlands, ISBN: 90-804551-6-4, pp. 63-70, 1999.